
AFRL-RB-WP-TP-2009-3218

# REVISITING THE NONLINEAR RESPONSE OF A PLATE TO ACOUSTIC LOADING (POSTPRINT)

**Joseph J. Hollkamp, Robert W. Gordon, and Timothy J. Beberniss**

**Structural Mechanics Branch**
**Structures Division**

**APRIL 2008**



**AIR FORCE RESEARCH LABORATORY**
**AIR VEHICLES DIRECTORATE**
**WRIGHT-PATTERSON AIR FORCE BASE, OH 45433-7542**
**AIR FORCE MATERIEL COMMAND**
**UNITED STATES AIR FORCE**

# REPORT DOCUMENTATION PAGE

*Form Approved*
*OMB No. 0704-0188*



| 1. REPORT DATE *(DD-MM-YY)* | 2. REPORT TYPE | 3. DATES COVERED *(From - To)* |
|---|---|---|
| April 2008 | Conference Paper Postprint | 01 January 2007 – 28 February 2008 |

**4. TITLE AND SUBTITLE**
REVISITING THE NONLINEAR RESPONSE OF A PLATE TO ACOUSTIC LOADING (POSTPRINT)

**5a. CONTRACT NUMBER**
In-house

**5b. GRANT NUMBER**

**5c. PROGRAM ELEMENT NUMBER**
62201F

**6. AUTHOR(S)**
Joseph J. Hollkamp, Robert W. Gordon, and Timothy J. Beberniss

**5d. PROJECT NUMBER**
A083

**5e. TASK NUMBER**

**5f. WORK UNIT NUMBER**
0G

**7. PERFORMING ORGANIZATION NAME(S) AND ADDRESS(ES)**
Structural Mechanics Branch (AFRL/RBSM)
Structures Division
Air Force Research Laboratory, Air Vehicles Directorate
Wright-Patterson Air Force Base, OH 45433-7542
Air Force Materiel Command, United States Air Force

**8. PERFORMING ORGANIZATION REPORT NUMBER**
AFRL-RB-WP-TP-2009-3218

**9. SPONSORING/MONITORING AGENCY NAME(S) AND ADDRESS(ES)**
Air Force Research Laboratory
Air Vehicles Directorate
Wright-Patterson Air Force Base, OH 45433-7542
Air Force Materiel Command
United States Air Force

**10. SPONSORING/MONITORING AGENCY ACRONYM(S)**
AFRL/RBSM

**11. SPONSORING/MONITORING AGENCY REPORT NUMBER(S)**
AFRL-RB-WP-TP-2009-3218

**12. DISTRIBUTION/AVAILABILITY STATEMENT**
Approved for public release; distribution unlimited.

**13. SUPPLEMENTARY NOTES**
Conference paper published in the Proceedings of the 49th AIAA/ASME/ASCE/AHS/ASC Structures, Structural Dynamics, and Materials Conference, 7 - 10 April 2008, Schaumburg, IL.

PAO Case Number: WPAFB 08-0125; Clearance Date: 23 Jan 2008. Report contains color.



**14. ABSTRACT**
Accurate prediction of the structural response of stiffened aircraft skins to acoustic loading is necessary for the design of future Air Force vehicles. Response prediction requires time integration of nonlinear models. Recently, methods have emerged where a nonlinear finite element model is reduced to a low-order system of nonlinear equations to better enable the computations. Well-characterized experiments are needed to validate these methods. In a previous study, experimental data from a thin rectangular plate subjected to acoustic loading were compared to model predictions. Poor agreement between the model predictions and the experimental data raised questions concerning the coupling between the structure and the acoustics. The experiment is repeated in this study with modifications to eliminate an acoustic resonance and better observe the structural/acoustic interaction. The results confirm that the modeling methods capture the structural mechanics of the problem, but lack the necessary coupling with the acoustic medium.

**15. SUBJECT TERMS**

| 16. SECURITY CLASSIFICATION OF: | | | 17. LIMITATION OF ABSTRACT: | 18. NUMBER OF PAGES | 19a. NAME OF RESPONSIBLE PERSON (Monitor) |
|---|---|---|---|---|---|
| a. REPORT | b. ABSTRACT | c. THIS PAGE | | | Robert W. Gordon |
| Unclassified | Unclassified | Unclassified | SAR | 18 | 19b. TELEPHONE NUMBER *(Include Area Code)* N/A |

**Standard Form 298 (Rev. 8-98)**
Prescribed by ANSI Std. Z39-18

AIAA 2008-2233

# Revisiting the Nonlinear Response of a Plate to Acoustic Loading

Joseph J. Hollkamp,[1] Robert W. Gordon,[1] and Timothy J. Beberniss[2]
*Air Force Research Laboratory, Wright-Patterson Air Force Base, Ohio, 45433*

**Accurate prediction of the structural response of stiffened aircraft skins to acoustic loading is necessary for the design of future Air Force vehicles. Response prediction requires time integration of nonlinear models. Recently, methods have emerged where a nonlinear finite element model is reduced to a low-order system of nonlinear equations to better enable the computations. Well-characterized experiments are needed to validate these methods. In a previous study, experimental data from a thin rectangular plate subjected to acoustic loading were compared to model predictions. Poor agreement between the model predictions and the experimental data raised questions concerning the coupling between the structure and the acoustics. The experiment is repeated in this study with modifications to eliminate an acoustic resonance and better observe the structural/acoustic interaction. The results confirm that the modeling methods capture the structural mechanics of the problem, but lack the necessary coupling with the acoustic medium.**

## Nomenclature

| | | |
|---|---|---|
| $A_r(i,j,k)$ | = | cubic stiffness in the nonlinear stiffness function |
| $\bar{\boldsymbol{C}}$ | = | damping matrix (generalized coordinates) |
| $\boldsymbol{f}(t)$ | = | applied force vector (physical coordinates) |
| $f$ | = | resonant frequency in Hz |
| $\boldsymbol{K}$, $\bar{\boldsymbol{K}}$ | = | stiffness matrices (physical and generalized coordinates) |
| ***K1, K2*** | = | quadratic and cubic stiffness matrices (physical coordinates) |
| $\boldsymbol{M}$ | = | mass matrix (physical coordinates) |
| $\boldsymbol{p}$ | = | the response vector (generalized coordinates) |
| $\boldsymbol{T}$ | = | a transformation matrix, the columns of which are the basis vectors |
| $t$ | = | time |
| $\boldsymbol{w}$ | = | the response vector (physical coordinates) |
| $\boldsymbol{\phi}_i$, $\boldsymbol{\Phi}$ | = | mode shape vector and mode shape matrix |
| $\boldsymbol{\theta}$ | = | nonlinear internal force vector (generalized coordinates) |
| $\omega$ | = | resonant frequency in radians/sec |
| $\zeta$ | = | damping ratio |

## I. Introduction

FUTURE Air Force vehicles will require structures that can withstand extreme environments. Prediction of the dynamic responses to acoustic loading will be necessary to design fatigue tolerant structures. Response prediction is difficult using traditional finite element modeling, since the acoustic loading is random and the response is nonlinear. The nonlinearity necessitates a time integration of the equations of motion, and the random nature necessitates long time records to form statistical averages. Direct integration of large nonlinear finite element models for long time records is unattractive. Several methods have been developed to transform the finite element model into a reduced-order set of equations.[1-5] These methods use a modal model augmented with nonlinear stiffness terms. The models offer the accuracy of a nonlinear finite element model with the computational efficiency of a modal model.

[1] Senior Aerospace Engineer, AFRL/RBSM.
[2] Aerospace Engineer, AFRL/RBSM.

The recent development of reduced order methods has generated the need to validate and verify the accuracy of the methods. Comparisons have been made between reduced-order predictions and full finite element model results.[1,2,4] The numerical comparisons have proven that the reduced-order models can replace a full finite element model. However, validation with experimental data is needed to ensure that the methods capture all the significant physics of the problem. In a recent experiment, a clamped plate was subjected to random base motion while on a shaker.[6] Comparisons between the predictions and experimental results were very good and improved significantly when nonlinear damping terms were added to the first modal equation. The physical mechanism producing the apparent nonlinear damping was not identified but it was speculated to be acoustic radiation. In a subsequent study, the structure was tested in a vacuum chamber while again subjected to random base motion. In a near vacuum state, the response of the structure could be predicted accurately without the addition of the nonlinear damping terms.[7] That study provided an excellent validation of the reduced-order model approach; however it occurred in the absence of air.

The validation experiments continued with testing of the same test article in an acoustic progressive-wave facility.[8] Comparisons between predictions and experimental results were initially only fair, but were improved significantly with two adjustments to the model. The first adjustment was the use of a measured differential pressure loading in lieu of the pressure in the progressive-wave facility. In the experiments, a microphone was set up behind the plate to measure the acoustic pressure. For some frequency ranges, the measured pressure behind the test article exceeded the acoustic loading in the progressive-wave facility. The difference between the two pressures was applied as the acoustic loading in the model. The second adjustment was a significant increase in the damping of the first mode. The damping in the first mode was increased from 0.5% to 5% of critical. Adding modal damping is a convenient way to model attenuation by some mechanism. The apparent attenuation could have been due to a transfer of energy to unmodeled modes or the transfer of energy to acoustic radiation. However, a damping value of 5% is a dramatic increase in the damping.

The apparent coupling of the acoustic field with the response of the structure in the previous experiments suggests that the models lacked relevant physics. Specifically, the models did not model the air surrounding the test article. That is, the reduced-order models were estimated from finite element models that were purely structural. Inclusion of the acoustic medium in the physical model is a computationally expensive proposition. The authors are not aware of any studies in which a reduced-order model incorporates both structural nonlinearity and the acoustic medium. In this paper, results from a second set of acoustic experiments are presented in an effort to answer whether the acoustic medium should be modeled.

## II. Reduced-Order Models

In this section, the reduced-order modeling approach known as the implicit condensation and expansion method (ICE) is summarized. More details can be found in the literature.[4] Finite element modeling of the nonlinear dynamic problem results in the nonlinear equations of motion

$$\boldsymbol{M}\ddot{\boldsymbol{w}} + [\boldsymbol{K}+\boldsymbol{K1}(\boldsymbol{w})+\boldsymbol{K2}(\boldsymbol{w},\boldsymbol{w})]\boldsymbol{w} = \boldsymbol{f}(t), \tag{1}$$

where $\boldsymbol{M}$ is the mass matrix, $\boldsymbol{K}$ is linear stiffness matrix, $\boldsymbol{w}$ is the displacement vector, and $\boldsymbol{f}(t)$ is a vector of external time-varying forces. The quadratic nonlinear stiffness matrix, $\boldsymbol{K1}$, is a linear function of the nodal displacements and the cubic nonlinear stiffness matrix, $\boldsymbol{K2}$, is a quadratic function of the nodal displacements. All of the quantities are in physical coordinates. Note that the finite element model is a purely structural model. The acoustic medium is not modeled. Acoustic effects enter the model only as an excitation pressure that is modeled as an external force.

The equations of motion can be transformed into generalized coordinates by selection of any suitable transformation matrix, $\boldsymbol{T}$,

$$\boldsymbol{w} = \boldsymbol{T}\,\boldsymbol{p}\,, \tag{2}$$

where $\boldsymbol{p}$ is a vector of generalized displacements or amplitudes. The columns of $\boldsymbol{T}$ are basis vectors. A common choice for the basis vectors is a truncated set of the modal vectors

$$\boldsymbol{T} = \boldsymbol{\Phi} = [\boldsymbol{\phi}_1\, \boldsymbol{\phi}_2 \ldots \boldsymbol{\phi}_n]. \tag{3}$$

Applying the modal transformation, the reduced equations of motion become

$$\ddot{\boldsymbol{p}} + \bar{\boldsymbol{C}}\,\dot{\boldsymbol{p}} + \bar{\boldsymbol{K}}\boldsymbol{p} + \boldsymbol{\theta}(p_1, p_2, \ldots, p_n) = \boldsymbol{\Phi}^T \boldsymbol{f}(t), \tag{4}$$

where

$$\bar{\boldsymbol{K}} = diag(\omega_1^2, \omega_2^2, \ldots, \omega_n^2), \tag{5}$$

and $\omega_i$ are the resonant frequencies of the modes included in the model. A damping matrix, $\bar{\boldsymbol{C}}$, has been introduced into the equations at this point. The damping matrix is usually assumed to be diagonal.

The nonlinearity appears as a vector function, $\boldsymbol{\theta}$. The equations are coupled solely through the nonlinear function. The form of the nonlinear function depends on the reduction method. In the ICE method, the basis vectors are the set of structural bending modes directly excited by the acoustic loading. Membrane modes are not explicitly included in the basis vectors. The form of the nonlinear function used in this paper is

$$\theta_r = \sum_{i=1}^{n} A_r(i,i,i)p_i^3 + \sum_{i=1}^{n-1}\sum_{j=i+1}^{n} \{A_r(i,i,j)p_i^2 p_j + A_r(i,j,j)p_i p_j^2\}, \tag{6}$$

for the $r$-th equation. The nonlinear function is restricted to include only cubic stiffness terms. Terms coupling three modes directly are neglected. The nonlinear function could have included quadratic terms, but these terms are negligible for a flat structure like the one used in this study. The coefficients of the nonlinear function are estimated from the results of a set of nonlinear static solutions obtained from a finite element code. Scaled combinations of the basis vectors are used as loads for the nonlinear static solutions.

Membrane modes are not required in the basis set, since the nonlinear effects of the membrane stretching appear in the static solutions. When the model coefficients are estimated, the stretching softens the cubic coefficients in the bending mode equations. In this manner, the membrane effects are implicitly included in the model. The model can be integrated to predict the modal bending amplitudes. Physical displacements that are spanned by the bending modes can be predicted. Physical membrane displacements are also needed for strain computation, but these displacements are not spanned by the bending modes. In the ICE method, a separate membrane basis set is estimated from the nonlinear static solutions. The membrane modal amplitudes are synthesized from the bending modal amplitudes and transformed into physical membrane displacements using the estimated membrane basis. The complete displacement field is thus available to accurately compute element strains using the finite element strain-displacement relationships.

## III. The Experimental Setup

In retrospect, the acoustic test and reduced-order model reported in the previous study[8] had significant flaws. First, the test article was mounted in the acoustic progressive wave facility in such a way that a semi-enclosed cavity existed behind it. This cavity resulted in an acoustic resonance that appeared as a resonant peak in the power spectral density (PSD) of the displacement of the test article. In addition, it was assumed that the acoustic pressure in the facility duct would not be affected by the test article. As a result, pressure measurements were taken only at the bottom of the duct and not near the surface of the test article. Finally, modal damping values used in the reduced-order model of the test article were measured before the test article was installed in the duct rather than after it was installed. The study presented here was conducted to correct these flaws and provide a more valid comparison between the model and experimental results.

The test article used in this study is the framed plate that was used in the previous experiments.[6-8] The test article was an aluminum alloy plate 0.0195 inches thick adhesively bonded between two aluminum alloy frames. The "framed" area of the plate measured 7 inches by 9 inches. The plate and frames were fabricated from 2024-T3 aluminum alloy with Young's modulus of $10.4\times10^6$ psi, a density of $2.59\times10^{-4}$ lb-sec$^2$/inch$^4$ and a Poisson's ratio of 0.33. The frames had a 1-inch by 1.5-inch "L" cross-section with a 0.25-inch-thick web and flange. The plate was bonded between the frames with Hysol® EA9320NA epoxy paste adhesive. The nominal bond line thickness was 0.005 inches. Four steel flexures were bolted to the frame flange at the center of each side. The blade-like flexures were each 1 inch by 3 inches by 0.1 inches. The flexures were flexible in bending, which allowed the test article to expand due to changes in temperature without building up significant in-plane stress. A photograph of the plate, frame, and flexures are shown in Fig. 1.

**Figure 1. The test article shown mounted on flexures with a solid mounting plate.**

Figure 1 shows the test article configuration used in previous experiments.[6-8] A thick mounting plate was located directly behind the test article. With the test article and mounting plate installed in the test facility, a semi-enclosed cavity was formed behind the test article. This caused a Helmholtz resonator which was acoustically coupled to the test article. In the current experiment, the mounting plate was redesigned as a larger plate with a large cut-out directly behind the test article. This configuration is shown in Fig. 2.

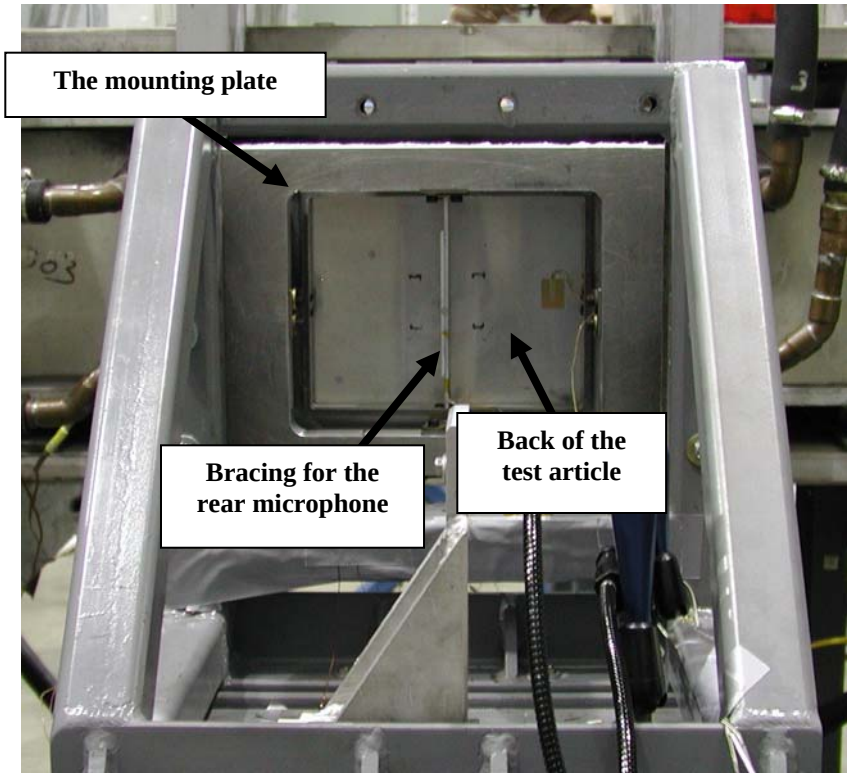


**Figure 2: The test article on a facility cart using a mounting plate with a rectangular cut out.**

The test article mounting plate was bolted to a rigid, massive cart as shown in Fig. 2. Attached to the front of the cart was a thick adapter plate. The adapter plate surrounded the test article so that when the cart was rolled into place in the acoustic facility, one side of the test article and the adapter plate became part of the facility side wall for the acoustic test. A gap of approximately 0.125 inches was left between the test article and the adapter plate to isolate the test article from any vibration from the adapter plate or the facility sidewall. These gaps were sealed with duct tape to minimize the amount of noise transmitted through them.

A modal test was performed on the test article before it was installed in the facility. Resonant frequencies, mode shapes and modal damping ratios were identified by exciting the test article with a 0-800 Hz low-level random acoustic signal. The excitation was generated by an acoustic driver with a 1.5-inch diameter tubular horn aimed at the back of the test article. Displacements of the plate were measured on a 7 by 9 rectangular grid (covering a 6-inch by 8-inch area) using a laser vibrometer. The temperature of the plate and frame were measured with thermocouples. The temperature difference between the plate and frame ranged from 0.0ºF to 0.1ºF during the modal tests. Frequency response functions (FRF's) were generated from the input signal to the acoustic driver and the measured displacement for each of the measurement points. Modal parameters were identified from the FRF's. The identified mode shapes are shown in Fig. 3. The coordinate directions are also shown in Fig. 3. The naming convention for the mode shapes is (*m*,*n*), where *m* and *n* denote the number of anti-nodes in the *x* and *y*-directions, respectively.

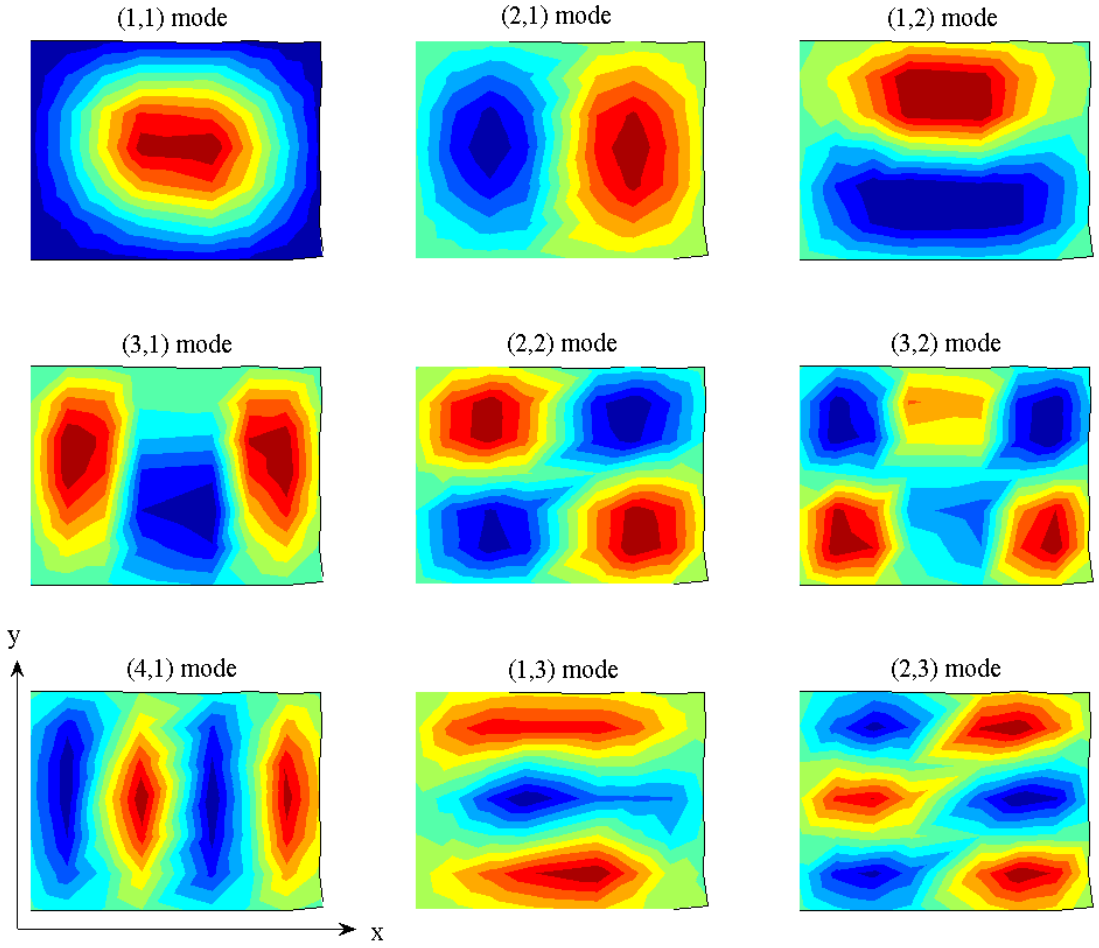


**Figure 3: Experimental measured mode shapes of the plate area of the test article.**

There were three symmetric modes in the 75-625 Hz frequency range of interest. These were the (1,1), (3,1), and (1,3) modes. If the acoustic loading was spatially uniform (i.e. the pressure did not vary across the test article), only these three modes would be directly excited. Ideally, the progressive-wave facility produces planar waves that have a grazing incidence with the test article. Thus, the acoustic loading is a traveling wave in the *x*-direction. The (2,1), (4,1), and (2,3) modes should be excited by the traveling wave along with the three symmetric modes.

When installed in the acoustic facility, the surface of the test article was flush with the sidewall of the progressive wave facility. A photograph of the facility with the test article installed is shown in Fig. 4. The acoustic source in this test was a single modified Wyle WAS 3000 airstream modulator. The modulator chops the flow of high pressure air to generate sound. The modulator was connected by a transition horn to a constant cross section duct that was six feet long and one foot square. The other end of the wave tube was attached to a horned shaped termination section (not shown in the photograph). Ideally, the facility produces a traveling plane wave. The wave propagation direction for the traveling wave is from right to left in Fig. 4. The propagation direction for the mode shapes shown in Fig. 3 is opposite, from left-to-right (i.e. the positive *x*-direction) since these mode shapes were measured on the front of the test article.

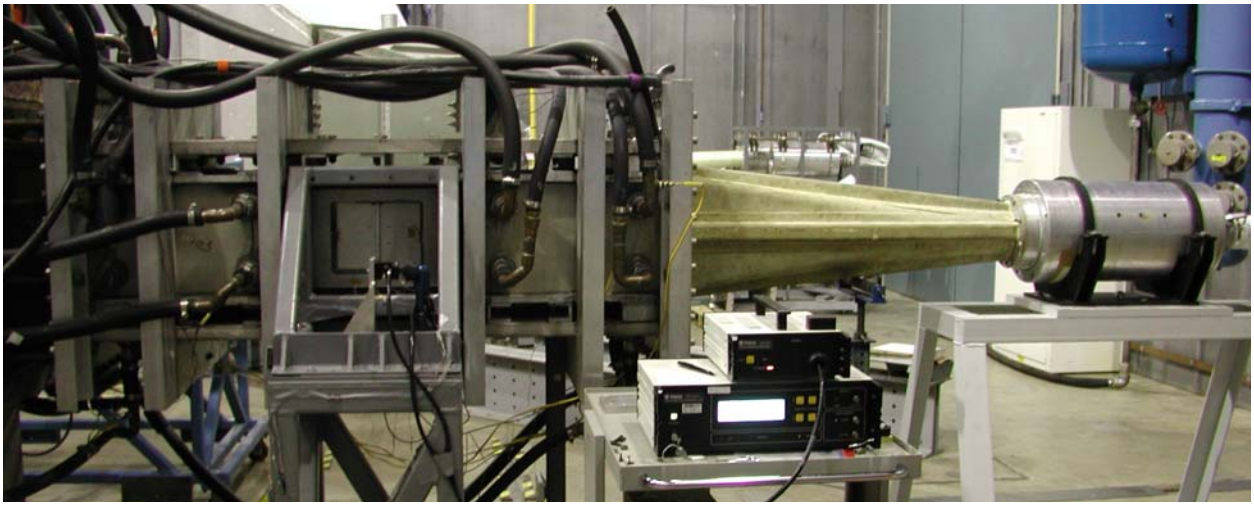

**Figure 4. The progressive-wave facility with the test article installed.**

A single-input single-output feedback controller is used with a reference microphone to control the input to the modulator to produce a random, normally distributed, spectrally controlled, sound pressure. The reference microphone was located at the bottom center of the duct, directly in front of the center of the test article. For this test, the plate was excited with a random acoustic signal in a 75-625 Hz band with overall sound pressure levels (SPL) of 122, 128, 134, and 140 dB at the reference microphone. These sound pressure levels are considerably lower than those used in a typical sonic fatigue test. However, the test article was much thinner (0.02 inches) than typical aircraft skin (0.040-0.10 inches) so that it would have nonlinear response at lower excitation levels.

Acoustic pressure was measured at five locations in all tests. Kulite LQ-125-5SG pressure transducers (microphones) were used. The reference microphone was located directly in front of the center of the test article, centered on the floor of the duct. This microphone was six inches below and six inches in front of the center of the test article. A second microphone was installed on the floor of the duct 18 inches upstream from the reference microphone. The third microphone was installed behind the test article, on the cutout of the mounting plate. That microphone was 3.5 inches behind the test article, 2.5 inches downstream from the center of the test article. Two additional microphones were used in this study. One measured the pressure 0.5 inches in front of the center of the test article and another measured the pressure 0.5 inches behind it. Ideally, the two additional microphones could have been located on the plate of the test article. However, since the plate vibrates during the experiment and the microphones were sensitive to axial vibration, it was decided to mount the additional microphones on added bracing. The bracing on each side consisted of two aluminum beams bonded together with ISD-112 viscoelastic adhesive. The viscoelastic material provided damping to reduce vibration of the bracing. The bracing was bonded to the frame of the test article with epoxy. The bracing for the rear microphone is shown in Fig. 2. The microphones were mounted on bracing so that they faced toward the test article. The bracing for the microphones was installed before any of the modal tests.

Displacements, velocities, and strains at selected locations on the test article were measured for all tests. Displacement and velocity were measured at a point near the center of the plate with a Polytec Model PSV-400 Vibrometer. The point was centered on the plate in the *y*-direction and was a quarter of an inch downstream from the center. Displacement and velocity were measured at second point with a Polytec Model OVF-512 Fiber Optic

Vibrometer. This point was 2.25 inches downstream from the upstream edge of the plate area and 1.5 inches above the lower edge of the plate area. Dynamic strains were measured with a pair of small resistive strain gages bonded to the center of the test article. The strain gages were oriented in the *x* and *y*-directions. The temperature of the plate area and the frame were measured with thermocouples and were continuously monitored during testing. The temperature of the plate area was 0.1ºF to 0.3ºF higher than the frame for all the acoustic tests. This was due to the fact that the air in the test section was somewhat warmer than the ambient air. Data records of the pressures, displacements, velocities, and strains were digitally sampled and stored for 100 seconds at each test level. The data was sampled at 50 kHz.

Two modal tests were conducted to measure the influence of the acoustic characteristics in the duct on the damping of the test article. A single-input single-output impact hammer modal test was conducted immediately before the test article was installed into the facility sidewall. A second impact hammer modal test was conducted immediately after installation. The estimated frequency and damping factors for the two tests are given in Table 1. There were no physical changes in the mounting of the test article between the uninstalled and the installed tests. The cart was simply rolled into place. The only difference was the boundary condition due to the acoustical field in the duct. Installation significantly affected the damping of several modes. The most significant effect occurred for the (1,1) mode, where the damping increased from roughly a quarter of a percent to almost two percent of critical! This large change in modal damping would have a very significant effect on the response. The effect of acoustic baffling on radiation damping is a likely cause of the observed damping increase. The influence of the duct acoustics also reduced the frequency of the (1,1) mode by nearly 3 Hz and increased the frequency of the (3,1) mode by 2.5 Hz.

**Table 1. Natural frequencies and modal damping ratios.**

| | Uninstalled | | Installed | | FE Model |
|---|---|---|---|---|---|
| Mode | $f$ (Hz) | $\zeta$ | $f$ (Hz) | $\zeta$ | $f$ (Hz) |
| (1,1) | 119.7 | 0.0024 | 117.0 | 0.019 | 113.4 |
| (2,1) | 199.7 | 0.0024 | 198.8 | 0.0027 | 195.7 |
| (1,2) | 286.5 | 0.0032 | 285.9 | 0.0054 | 264.5 |
| (3,1) | 322.6 | 0.0061 | 325.1 | 0.011 | 331.6 |
| (2,2) | 354.7 | 0.0027 | 354.2 | 0.0027 | 340.0 |
| (3,2) | 466.1 | 0.0033 | 465.4 | 0.0030 | 468.6 |
| (4,1) | 498.5 | 0.0038 | 497.3 | 0.010 | 519.2 |
| (1,3) | 512.5 | 0.0075 | 512.7 | 0.0054 | 498.6 |
| (2,3) | 581.1 | 0.0067 | 579.5 | 0.0055 | 571.0 |

## IV. Modeling

This section discusses the various model features used in the reduced-order models. The finite element model used to construct the reduced-order models is summarized. Modal basis selection and the manner in which the excitation is modeled are also discussed.

The reduced-order modeling approach requires that a finite element model be constructed. The finite element model was the same model as used in a previous study.[8] The model explicitly included the plate, frames, adhesive, and flexures. The model used 4-noded shell elements for the plate and flexures and 8-noded solid elements for the frame and adhesive. A 1/4-inch by 1/4-inch mesh size was used for the plate. The total number of elements in the model was 6536. The 7-inch by 9-inch plate required only 1008 of those elements. The only boundary condition imposed on the model was to fix all degrees-of-freedom (DOF) at the ends of the flexures that attached to the mounting plate. The mass and stiffness of the strain gages, thermocouples, and wires were not included in the model. For simplicity, the microphone bracing was also not included. (A second finite element model revealed that the microphone bracing had minimal effect on both the frequencies and mode shapes.) No thermal loads were

applied to the model. The model was analyzed in ABAQUS. A normal modes analysis was performed. The natural frequencies for the first nine modes are listed in Table 1.

The first step in constructing the reduced-order models is to decide on the model basis. The basis vectors were selected from the analytical mode shapes. The spatial distribution of the acoustic excitation has to be considered in the selection. If a spatially uniform pressure is assumed, only the symmetric modes are directly excited. A three-mode model was built retaining the (1,1), (3,1) and (1,3) modes. However the acoustic excitation should be a plane wave with grazing incidence. The pressure appears on the plate as a random amplitude wave traveling in the *x*-direction. The traveling wave can directly excite the three symmetric modes. In addition, the traveling wave can directly excite modes that are anti-symmetric in the *x*-direction and symmetric in the *y*-direction. A six-mode model was built retaining the (2,1), (4,1), and (2,3) modes, as well as, the (1,1), (3,1), and (1,3) modes. The reduced-order models were generated from the finite element model using the ICE method implemented in Matlab. The nonlinear static solutions, used to construct the reduced-order models, were performed in ABAQUS. The three-mode model had three nonlinear differential equations. There were nine nonlinear stiffness terms in each equation. The six-mode model had six equations with 36 nonlinear stiffness terms in each equation.

The natural frequencies in the model correspond to those from the finite element model. In this paper, the experimentally measured frequencies will be used in lieu of the analytical frequencies. The change of frequencies would be difficult to do in a full finite element model but was easily accomplished in the reduced-order model. The experimentally measured damping was also used in the reduced-order model. This model update was done to remove minor tuning issues from the comparison, so that the major issues of structural-acoustic coupling could be focused on. Two sets of measured frequency and damping were recorded (listed in Table 1) both sets will be explored when comparing predictions to experimental data.

The next consideration is the modeling of the excitation. The acoustic excitation enters the model only as an acoustic pressure that is modeled as an external force. The excitation can be modeled as either uniform or traveling. The uniform pressure is often considered simply because it is easier to model. In the uniform case, the loading is simulated as a spatially uniform pressure. The amplitude of the pressure varies in time. The grazing incident wave in the facility is a traveling wave. In the traveling wave case, the pressure amplitude varies in time, is spatially uniform in *y*-direction, but varies in *x*-direction based upon the speed of the traveling wave. The scheme for simulating the traveling wave was adopted from the literature.[9] The measured time history of the excitation was used as the amplitude of either forcing scheme (more on this will be discussed later). Time integration was performed using the Newmark beta method. Time histories were generated for each of the acoustic levels. Each time history was a digital record 100 seconds long with a step size of 0.00002 seconds.

## V. Comparisons with Test Results

In this section, test results are presented and compared with predictions from a reduced-order model. Some of the model parameters were varied to improve agreement with test results. The parameters that were varied included the modal basis, modal damping ratios, and the form of the excitation. In addition to improving the agreement with test results, these model variations helped answer whether structural-acoustic coupling effects need to be included in the model.

The response will be examined using the displacement at the two measurement points. The first measurement point is 0.25 inches from the center of the panel. For convenience, the point will be referred to as the center location. The response at this measurement point will be dominated by the three symmetric modes. The other measurement location will be referred to as the off-center location.

Although data was experimentally acquired for four sound levels, for brevity, only the data for the highest and the lowest levels will be presented. The lowest level at 122 dB is the closest to linear response. Predicted response at this level should be dominated by linear parameters such as the natural frequencies and the damping values. The highest excitation level at 140 dB is highly nonlinear. At this level, the nonlinear stiffness effects should dominate the response.

The first response prediction case is a three-mode model with uniform pressure. The measured reference pressure time history is used as the excitation to this model. The uninstalled frequency and damping parameters are used in the model. Figures 5 and 6 show predicted displacement PSD's in comparison to test data for the two measurement locations. The predictions exhibit much more nonlinearity than the experimental data. The predicted peaks show too much nonlinear broadening. This is particularly true for the first mode. It is also evident from the off-center displacement in Fig. 6 that more than three modes are excited.

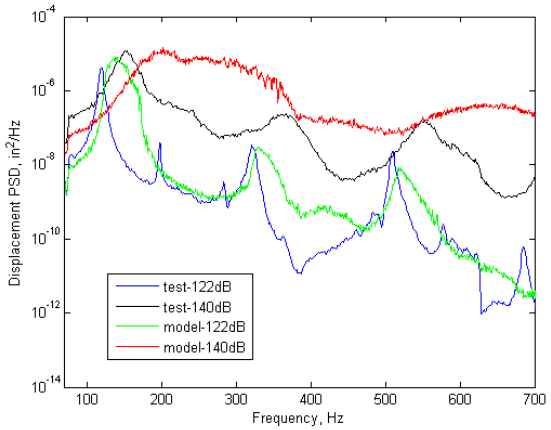


**Figure 5. Comparisons for the center location from a three-mode model with the uninstalled parameters driven by a random, spatially uniform pressure.**

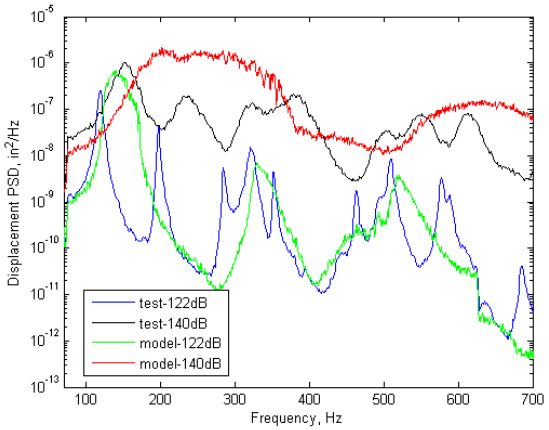


**Figure 6. Comparisons for the off-center location from a three-mode model with the uninstalled parameters driven by a random, spatially uniform pressure.**

Three changes were made to the model to improve the prediction. First, the six-mode model was used instead of the three-mode model. The additional three modes can not be excited by the uniform pressure. Therefore, the second change is that the excitation is modeled as a traveling wave. The third change is to increase the damping by using the installed damping parameters. The nonlinear broadening shown in the previous predictions should be reduced by an increase in damping. Installed modal frequencies were also used. Predicted displacement PSD's using the six-mode model are shown in Figs. 7-8. The low level model predictions in Fig. 7 confirm that the installed damping values are now more reasonable. Additional resonant peaks appear in the low level predictions in Fig. 8 indicative of the higher order model. Specifically, the (2,1) mode appears near 200 Hz and the (2,3) mode is evident near 580 Hz. The (4,1) mode should appear near 500 Hz, but is apparently masked by the (1,3) mode near 510 Hz. The high level predictions exhibit less nonlinearity than the previous predictions, but the first mode still exhibits a shift in natural frequency compared to the experimental data.

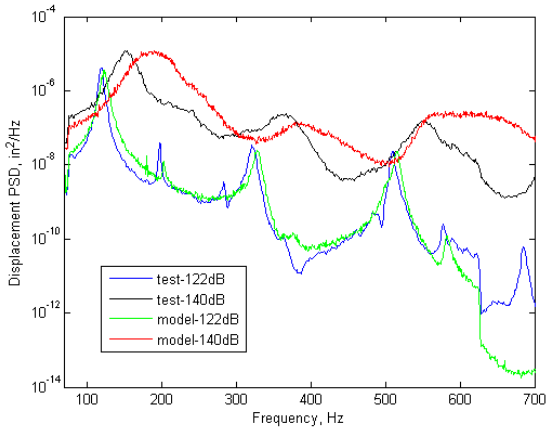


**Figure 7. Comparisons for the center location from a six-mode model with the installed parameters driven by a random, traveling pressure wave.**

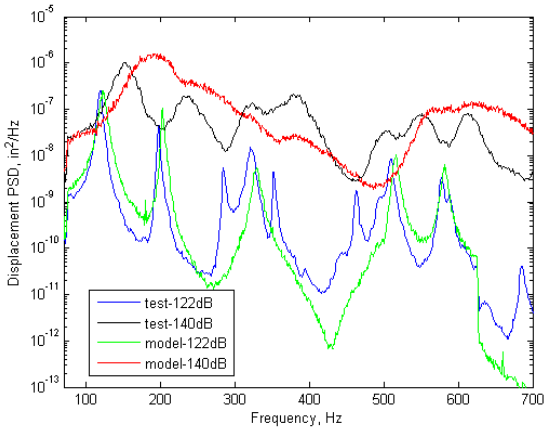


**Figure 8. Comparisons for the off-center location from a six-mode model with the installed parameters driven by a random, traveling pressure wave.**

The apparent excessive nonlinearity in the first mode peak could be due to several factors. In a previous study,[7] excellent agreement was obtained between a three-mode model and the test article in vacuum. Therefore, the possibility that the model's nonlinear parameters are inaccurate and provide too much hardening is discounted. A second factor that could cause the apparent excessive nonlinearity is a deviation of the acoustic excitation from the

flat spectrum measured at the reference microphone. The discrepancies encountered in the previous acoustic experiment[8] suggest that acoustic pressure at the plate surface may be different from the reference pressure.

The measured front, rear, and reference pressures for the low level case are shown in Fig. 9. The feedback controller forces the reference pressure spectrum to be flat. However, the pressure in front of the plate has a significant peak that occurs at the (1,1) mode frequency. The pressure behind the plate also has this same peak. Also note that the acoustic cavity resonance that occurred in the previous experiment[8] is gone. Clearly, there still are structural-acoustic coupling effects. The resulting differential pressure (the front pressure minus the back pressure) is plotted in Fig. 10. The spectrum level of the differential pressure is more than an order of magnitude higher than the reference at frequencies near the first structural modal frequency. Figures 11 and 12 show the high level pressures. The difference between the differential and the reference spectrums are lower for this case, but are still significant. Note that for both test levels, the differential pressure exceeds the reference pressure near the first resonance, but the spectrum of the differential is lower than the reference immediately after the resonance.

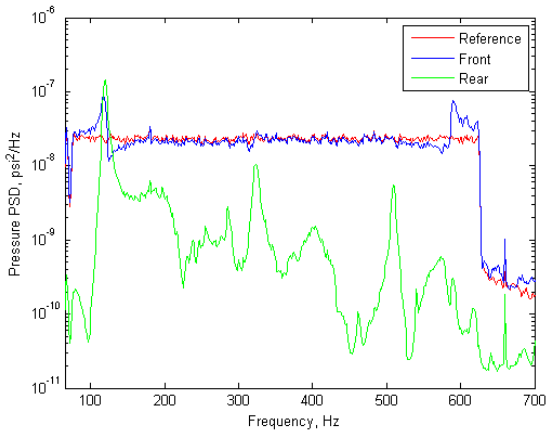


**Figure 9. Measured pressure spectra for the 122dB test level.**

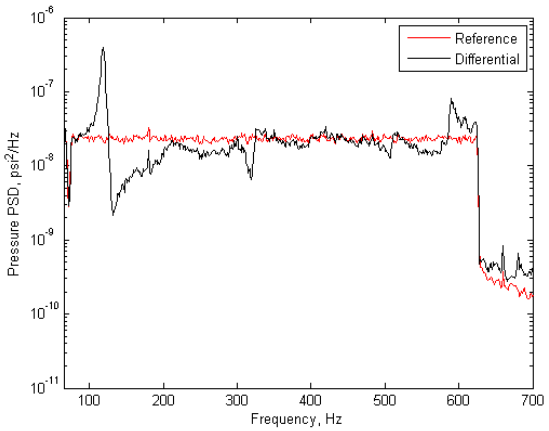


**Figure 10. The reference and the differential pressure spectra for the 122dB test level.**

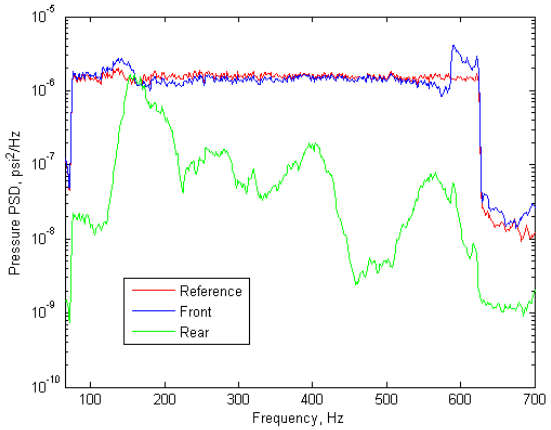


**Figure 11. Measured pressure spectra for the 140dB test level.**

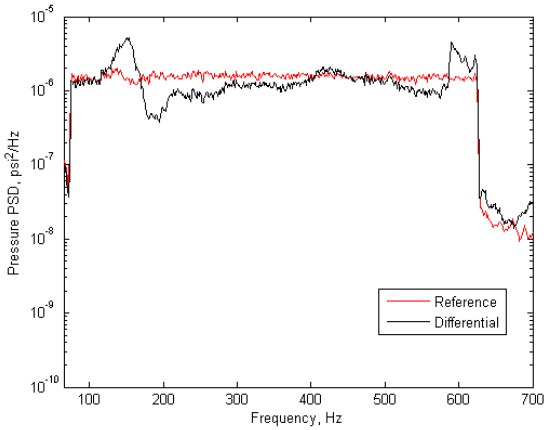


**Figure 12. The reference and the differential pressure spectra for the 140dB test level.**

To further improve the model, the excitation time history was changed from the reference pressure to the differential pressure. The excitation was still modeled as a traveling wave. Note that the component of the pressure field due to the structural response was probably not a traveling wave. However the traveling and stationary components could not be separated and a traveling wave was necessary to excite all the modes. The predicted displacement PSD's for the model with traveling wave differential pressure excitation are shown in Figs. 13-14. The predicted response for the center location agrees very well with the experiment for both excitation levels. The prediction for the off-center location is also very good with the exception of the response of the modes not included in the model.

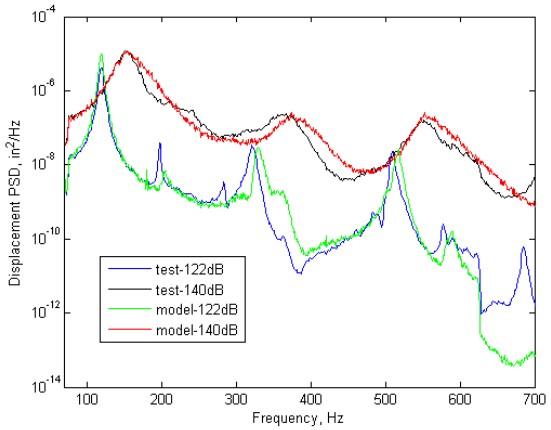


**Figure 13. Comparisons for the center location from a six-mode model with the installed parameters driven by a traveling differential pressure.**

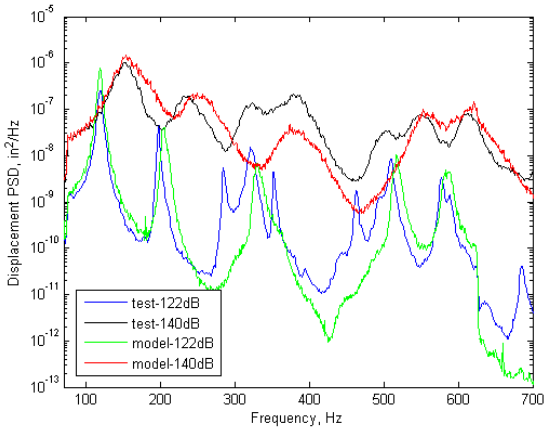


**Figure 14. Comparisons for the off-center location from a six-mode model with the installed parameters driven by a traveling differential pressure.**

Additional modes could have been added to the reduced-order model in an effort to improve the prediction. The additional modes available in the finite element model, the (1,2), (2,2), and (3,2) modes, are anti-symmetric in the *y*-direction. These modes can not be directly excited by a pressure field that is symmetric in the *y*-direction, as exists in the duct. The modes could possibly be *parametrically* excited by the other modes through nonlinear coupling terms. To test this effect, a nine-mode model was constructed. However, the nine-mode model gave identical results to six-mode model. The fact that additional modes appear in Fig. 14 is probably due to the fact that the actual test article is not perfectly symmetric in the *y*-direction.

## VI. Summary and Conclusions

Experiments are needed to validate reduced-order modeling methods for the structural-acoustic response problem. In a previous study,[8] experimental data from a thin rectangular plate subjected to acoustic loading were compared to model predictions. Poor agreement between model predictions and the experimental data raised questions concerning the coupling between the structure and the air. The experiment was repeated in this study with modifications to better observe the structural/acoustic interaction. The results confirm that the modeling methods capture the structural mechanics of the problem, but lack the necessary coupling with the acoustic medium.

Experiments were conducted in an acoustic facility to investigate the importance of structural-acoustic coupling. The test article consisted of a thin plate bonded between two halves of an aluminum frame designed to provide nearly-clamped boundary conditions. The test article was used in previously and has been well-characterized.[6-8] In the present study, the test article was mounted as part of the sidewall of a progressive wave tube and was subjected to high-intensity acoustic traveling wave loading. There were two indications in the test data that strong structural-acoustic coupling was present in the experiment. First, the modal damping of the test article changed when it was inserted into the facility. The change in the first mode was dramatic, increasing from approximately 0.25% of critical to approximately 2%. These changes could not be attributed to any structural difference. Second, the pressure immediately in front of the test article contained a peak in the spectrum that corresponded to the first structural mode. Clearly, the structural response interacted with the acoustic loading.

The data from the test were compared to predictions from reduced-order models. A finite element model of the test article was used to construct reduced-order models. The finite element model contained only structural elements. The predictions compared well to the data only when the increased damping values where used and the measured differential pressure was used as the excitation force. In effect, the model was adjusted to compensate for the structural-acoustic interactions by modifying the parameters and the input to the model.

The results show that structural-acoustic coupling is important. The model could predict the test data, if measured values were used. However, the model could not predict the response without prior knowledge of the effects of the structural-acoustic interaction. Therefore, reduced-order models built from structural finite element models may not be adequate to predict the acoustic response of thin panels. Coupling with an acoustic medium may need to be included in the model A caveat to these observations is that the test article used in this study was extremely thin and may not be representative of typical aircraft structures with thicker skins.

## VII. References

[1]McEwan, M.I., Wright, J.R., Cooper, J.E., and Leung, A.Y.T., "A Finite Element/Modal Technique for Nonlinear Plate and Stiffened Panel Response Prediction," AIAA-2001-1595, 2001.

[2]McEwan, M.I., "A Combined Modal/Finite Element Technique for the Non-Linear Dynamic Simulation of Aerospace Structures," Ph.D. Dissertation, School of Engineering, University of Manchester, Manchester, UK, 2001.

[3]Hollkamp J.J., Gordon R.W., and Spottswood S.M., "Nonlinear Modal Models for Sonic Fatigue Response Prediction: A Comparison of Methods," *J. of Sound and Vibration*, Vol. 284 (3-5), 2005, pp. 1145-1163.

[4]Hollkamp, J.J., and Gordon, R.W., "Modeling Membrane Displacements in the Sonic Fatigue Response Prediction Problem," AIAA-2005-2095, 2005.

[5]Muravyov, A.A., and Rizzi, S.A., "Determination of Nonlinear Stiffness with Application to Random Vibration of Geometrically Nonlinear Structures," *Computers and Structures*, Vol. 81, pp. 1513-1523, 2003.

[6]Gordon R.W. and Hollkamp J.J., "Nonlinear Response of a Clamped Plate to Random Excitation: a Well-Characterized Experiment," AIAA-2006-1924, 2006.

[7]Beberniss, T.J., Gordon R.W., and Hollkamp J.J., "The Effect of Air on the Nonlinear Response of a Plate," AIAA-2007-2085, 2007.

[8]Hollkamp J.J., Beberniss, T.J., and Gordon R.W., "The Nonlinear Response of a Plate to Acoustic Loading: Predictions and Experiments," AIAA-2006-1928, 2006.

[9]Mei C., and Moorthy J., "Numerical simulation of the nonlinear response of composite plates under combined thermal and acoustic loading," NASA-CR-197426, 1995.